Laboratori Nazionali di Frascati

LNF-92/104 (P)
3 Dicembre 1992

U. Gambardella, D. Di Gioacchino, V. Boffa, G. Paternò, S. Barbanera, F. Murtas:

CRITICAL CURRENTS IN NbZr SUPERCONDUCTING THIN FILMS

To be published on
IEEE Transation on Applied Superconducting

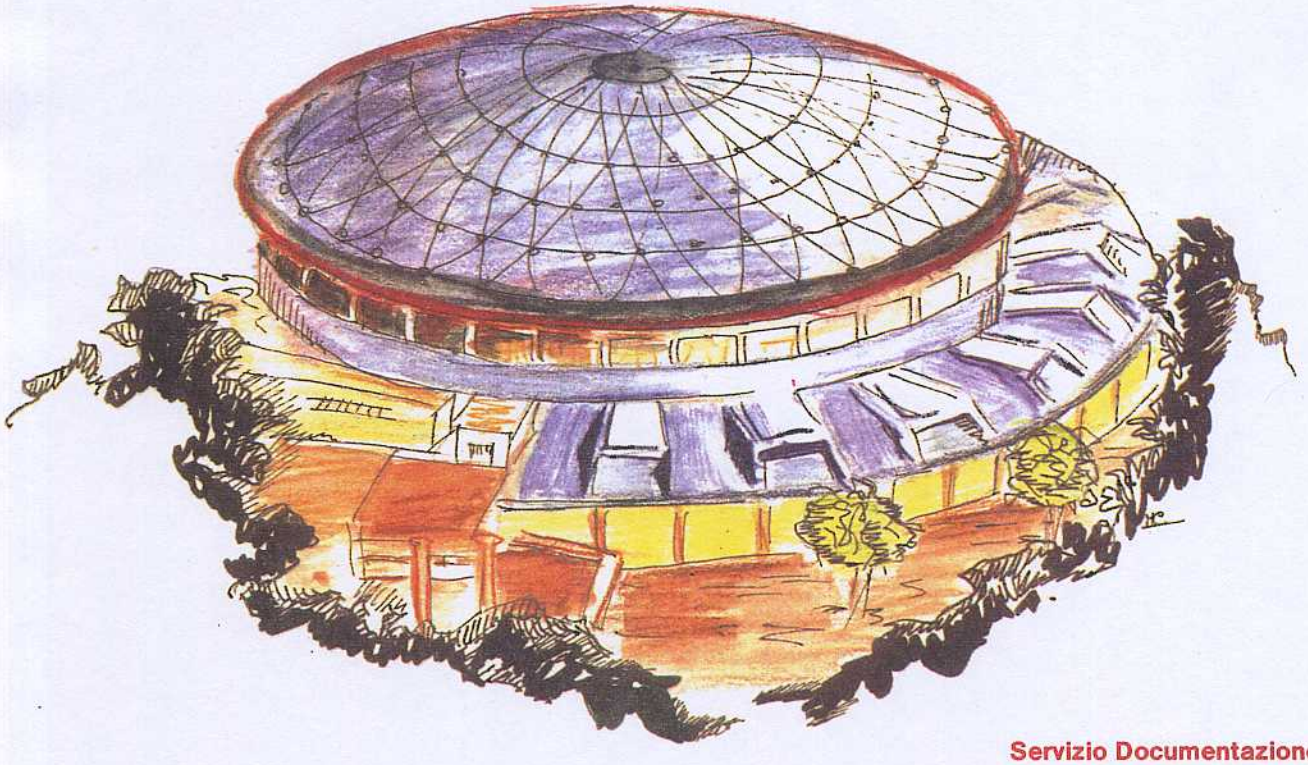

Servizio Documentazione
dei Laboratori Nazionali di Frascati
P.O. Box, 13 - 00044 Frascati (Italy)

INFN – Laboratori Nazionali di Frascati
Servizio Documentazione

LNF–92/104 (P)
3 Dicembre 1993

CRITICAL CURRENTS IN NbZr SUPERCONDUCTING THIN FILMS

U. Gambardella* , D. Di Gioacchino*, V. Boffa, G. Paternò, S. Barbanera+ , F. Murtas+
ENEA–CRE Frascati
Via E. Fermi 27, 00044RM Frascati (Roma) Italy

ABSTRACT

$Nb_{0.75}Zr_{0.25}$ thin films have not yet been investigated in all the features that may come from their higher critical temperature compared to other Nb alloys. In this work we present the fabrication of $Nb_{0.75}Zr_{0.25}$ thin films by sputtering which showed critical temperature as high as 10.5 K. We also present transport critical current measurements on $Nb_{0.75}Zr_{0.25}$ films whose geometries were photolitographically defined in the μm range. The measurement were performed as a function both of the temperature and of the magnetic field up to 6 Tesla. The temperature behavior is compared with the Kim–Anderson model, while the magnetic field behavior of the resulting pinning force has been compared with existing models.

I. INTRODUCTION

The $Nb_{0.75}Zr_{0.25}$ alloy has an high Ginzburg–Landau κ value [1], and a bulk critical temperature $T_c \approx 10.8$ K [2]. These features make it interesting for applications in superconducting devices at least where high magnetic fields are not relevant compared to the potential induced benefits due to a higher T_c, such as in RF superconducting devices. The literature reports very few data on $Nb_{0.75}Zr_{0.25}$ thin films [3–5] fabricated by sputter deposition and generally the reported T_c's are well below the bulk value, except in cases of high substrate temperatures during the film growth (>500 °C) and very high deposition rates [4]. Recently it has been reported [5] a $T_c \approx 10.2$ K for $Nb_{0.75}Zr_{0.25}$ thin films for which, by means of tunneling measurements, some parameters were also derived. Unfortunately further interesting properties are still missing, like the critical current density J_c behavior, necessary to study the pinning

---

* present address INFN-L.N.F., Frascati, Italy
+ CNR - I. E. S. S., Via Cineto Romano 42, 00156 Roma, Italy
Work partially supported by CNR under the Progetto Finalizzato "Superconductive and Cryogenic technologies".

force in $Nb_{0.75}Zr_{0.25}$ thin films. In the present work we outiline the sample fabrication, shaped as narrow thin film striplines (5–40) μm width, 2mm long, which allowed to obtain large J_c, higher than 10^6 A/cm^2 at 4.2 K, with low bias currents (less than 100 mA at the lowest temperature) in a wide temperature range. On these samples we recorded both resistive transitions in an applied magnetic field H and the J_c behavior as a function of both temperature T, in the range (4.2–9.5) K, and transverse magnetic field, from 0 to 5.8 Tesla. Experimental data are then used to estimate the superconducting parameters of the material, such as the upper critical field H_{c2} at T=0 K, and the intrinsic coherence length ξ_0.

Furthermore the zero– temperature transport critical current density J_0 is computed from the Anderson–Kim flux creep theory on pinning:

$$J = J_0 (1 - \gamma t - \beta t^2) \qquad (1)$$

where $t=T/T_c$, and the γ, β coefficients are estimated from experiments. Finally the J_c vs H curve are shortly discussed and the pinning force behavior is outlined. The possibility of some scaling law in different situations is suggested.

II. EXPERIMENT

We have realized the films by using both RF and DC sputtering from water cooled magnetron cathode, where a $Nb_{0.75}Zr_{0.25}$ target disc was welded. The films were grown on sapphire substrates whose holder was provided with an electrical heater. The base vacuum before depositions was typically less than 4×10^{-7} Torr, while the sputtering was performed in a pure Ar atmosphere in the 10^{-3} Torr range. A pre–sputtering always preceeded the deposition processes. Typical thicknesses were roughly 5000 Å and 2500 Å, respectively corresponding to 300 s and 150 s of deposition time. The substrate holder temperature was always 400 °C except for sample #17 which was not intentionally heated. After the film deposition we defined the sample geometry by photolithography. The excess film was removed by an ion milling process. Only sample #17 was chemically etched.

Table 1 – Geometrical and electrical properties of samples; *d* is the nominal thickness before patterning.

Sample	*d* [Å]	w [μm]	S [μm^2]	ρ_{11K} [μΩcm]	$\frac{R_{300K}}{R_{11K}}$
# 17	6500	16	10	43.7	1.42
# 25	5000	30	18	36.4	1.42
#29A	2600	15	4.4	34.2	n.a.
	3000	20	5.6	31.6	1.51
#29B	3500	5	2.1	53.2	1.51
	3500	15	4.9	41.2	1.47
	3500	20	6.3	36.8	1.46

The ion etching took place in a vacuum chamber provided with a 2.5 cm diameter ion gun where the 4 sccm flow of pure Ar gave rise to a pressure of 10^{-4} mbar. Typical energy was 600 eV, while the ion current was 50 mA. The distance between the gun and the sample was 10 cm; the gun axis was at 45° with respect to the film plane. The typical etching time was 5 min for a 6000 Å thick film. Lines as narrow as 5 μm with good homogeneity along the

2000 μm of length were realized. After the patterning process the cross sections of the striplines were measured with an alpha–step profilometer. Multiple measurements along a single line indicated a variation of ±2% of the cross sectional area. In Table 1 are summarized the main geometrical and electrical properties of some samples.

The characterization was performed in a He gas flow variable temperature cryostat provided with a superconducting magnet capable of generatint a uniform and constant field up 5.8 Tesla. The samples were fixed on a bulk copper sample holder with the bias current and the film plane perpendicular to the applied magnetic field. Both current and voltage leads were soft soldered with indium on the corresponding pads.

The resistive transitions were recorded with a typical (1–100) μA bias current, depending on the sample resistance, however low enough for not giving rise to self heating on current leads and contacts. The standard double voltage reading, with direct and inverse current flow, was adopted to neglect the fluctuating thermal emfs. The temperature was measured by means of a Lake Shore calibrated carbon glass resistor (CGR 1–2000), placed in close thermal contact with the sample, fed with 10 μA costant current, also with the double voltage reading technique. The residual resistivity ρ_n of our films ranged in the (30÷50) μΩ cm interval, the residual resistivity ratio RRR ≈1.5. The critical temperature T_c was typically (10.2±0.05) K, and for a 600 °C substrate temperature deposition, i.e. sample #31, we got T_c=10.5 K.

In Fig. 1 the resulting T_c measured from the resistive transitions recorded at different magnetic field values are reported as H_{c2} vs T.

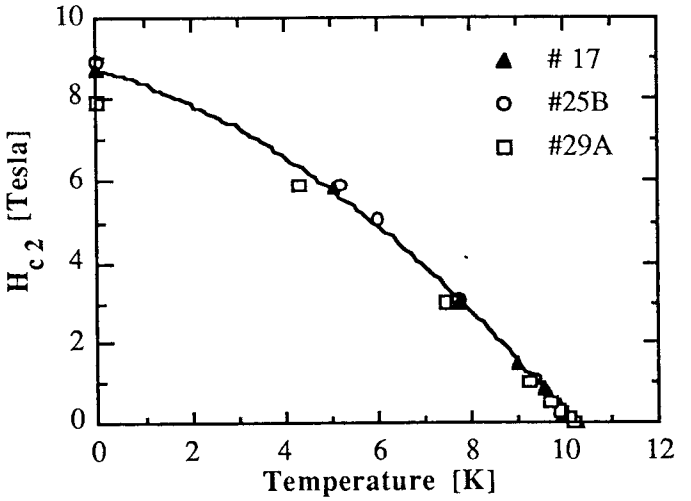

FIG. 1 – Upper critical field derived from resistive transition in transverse magnetic field. Zero temperature values are estimated with WHH theory.

Critical current measurement were made by using the same configuration. Current–voltage (I–V) characteristics of the films at temperatures between 4.2 K and 9.5 K were taken by accurate thermal regulation of the He gas flow, while at 4.2 K the samples were immersed into the LHe. To further minimize the self–heating effects on the current contacts the bias current was stepped from zero to a value below the critical one, and after the rate of increase was suitably adjusted to allow recording of the I–V curves. The voltage threshold criterion V_{th} to evaluate the critical current density J_c was typically 1 μV or 10 μV, corresponding to an

electrical field of 5 and 50 μV/cm respectively. The current which gave rise to a voltage within a window [$0.92*V_{th}<V<V_{th}$] neighboring the threshold voltage was recorded as the critical current value. In this way also an upper limit criterion for the voltage corresponding to the critical current was set. The differences between the critical currents recorded with V_{th}=1μV and V_{th}=10 μV were less than 20%, however not affecting the J_c behavior with either temperature or magnetic field.

In Fig. 2 the J_c vs t behavior is shown for two samples. Both samples exhibit the same behavior with different J_0.

In Fig. 3 some critical current density measurements as a function of the transverse magnetic field are shown; solid symbols refer to samples #17 (circles), #29A (rhombs), and # 29B (triangles), recorded at T=9.5 K, while open symbols refer to T=4.2 K.

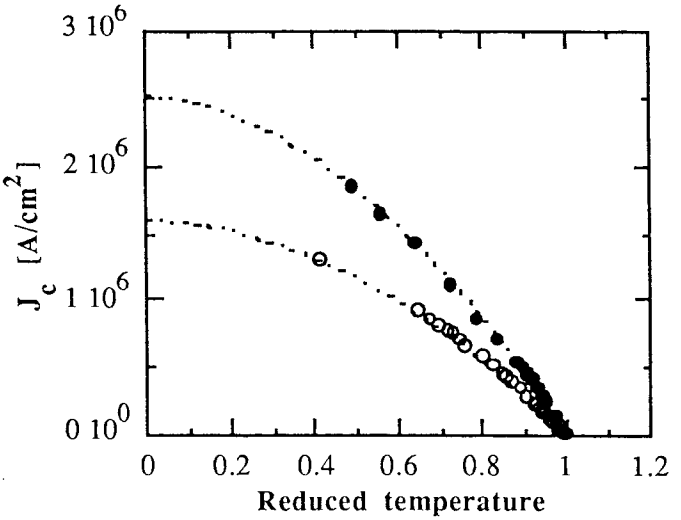

FIG. 2 – J_c vs t for samples #17 (open circles) and #25B (solid circles). Dotted lines are eq. 1 with γ=0.1 and β=0.9.

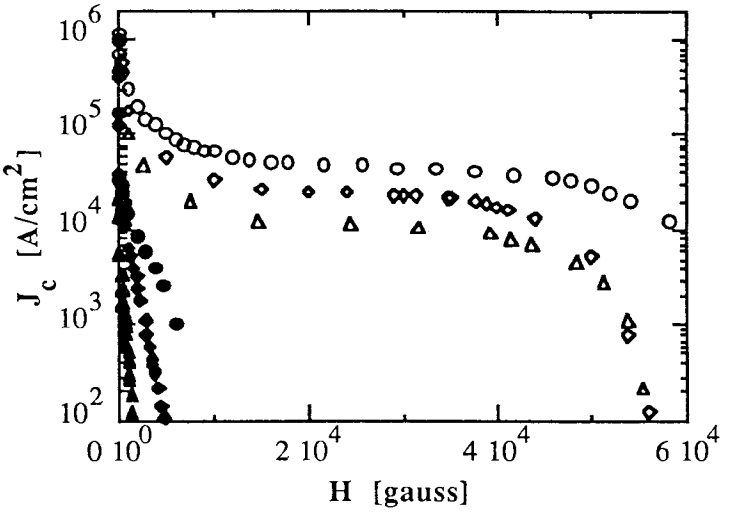

FIG. 3 – Critical current density behavior as a function of transverse magnetic field for samples #17 (circles), #29A (rhombs), and # 29B (triangles); solid symbols and open symbols were recorded at T=9.5 K and T=4.2 K respectively.

III. DISCUSSION

$H_{C2}(T)$ of $Nb_{0.75}Zr_{0.25}$ films is analyzed according to the WHH theory [6]. In Fig. 1 it is shown the $H_{C2}(T)$ behavior and the value $H_{C2}(0)$ comes from $H_{c2}(0)\approx 0.7[dH_{c2}(t)/dt]_{t=1}$. For the samples shown we have $H_{c2}(0)\approx 86.0\pm 6.8$ kG. This is about 15% lower than the reported bulk value $H_{c2}(0)\approx 100$ kG [7, 1], which however is comparable to the value of $H_{c2}(0)$ previously obtained on $Nb_{0.75}Zr_{0.25}$ films in a parallel magnetic field [8]. We attempt to estimate the intrinsic coherence length ξ_0 and the mean free path l from $H_{c2}(T)$. Being [9] $v_F\approx 5\times 10^7$ cm s^{-1} we compute $l\approx 6.7$Å and $\xi_0\approx 610$Å respectively from $H_{c2}\approx 3\times 10^4\ T_c/(v_F l)$ and $H_{c2}\approx \Phi_0/(2\pi\xi^2)$, where v_F and Φ_0 respectively are the Fermi velocity and the flux quantum. The l value is comparable to previuos results, while ξ_0 is quite different from the value obtained by tunneling measurements [5].

The agreement of $J_c(T)$ with the Anderson and Kim theory is satisfactory, as shown in Fig. 2. The values of $J_0(0)$ are comparable with reported values measured in bulk and films, as well as the β, γ coefficients.

The $J_c(H, T)$ curves are summarized in Fig.s 4 and 5 as the reduced pinning force F_p vs the reduced magnetic field h. In Fig. 4 the pinning force behavior is shown both near T_c and below $T_c/2$ for two different samples. We do not observe any scaling law [10] at least for $T\approx T_c$, but, in view of two well separated maxima at the two temperatures, there seems to be different pinning mechanisms. However analyzing the more complete temperature behavior of the maxima, reported in Fig. 5, it comes out that the first maximum at $h\approx 0.2$ is evident only for T=9.5K, and at T=8.5K a pronounced shift toward $h\approx 0.6$ is already present. Lowering the temperatures, T=6.5K, 5K, and 4.2K, induces only minor differences among the curves, whose maxima occur at $h\approx 0.6\div 0.7$. In this way, at lower temperatures, a pinning force scaling law seems effective. In any case the typical shearing behavior $F_p\sim h^{1/2}(1-h)^2$, for $h>0.6$, does not fit well our data.

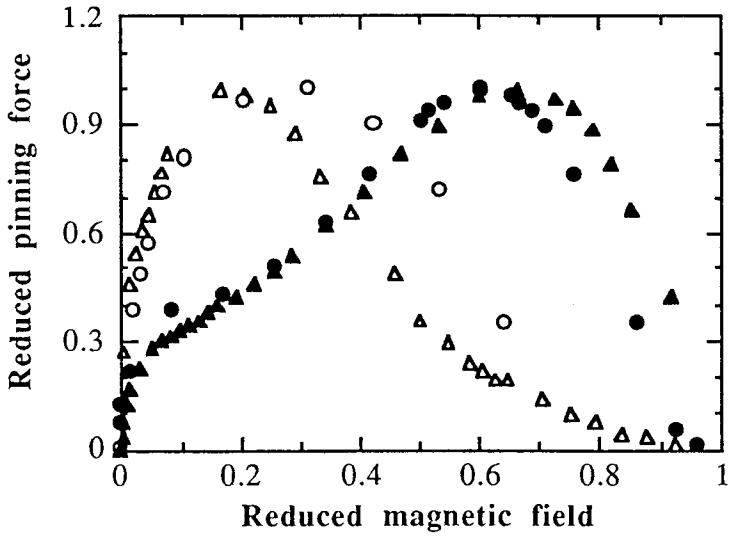

FIG. 4 – F_p vs h for sample #17 (circles) and #29A 20μm line (triangles) at T=9.5 K (open symbols) and T=4.2 K (solid symbols).

As a final remark on the pinning force in our $Nb_{0.75}Zr_{0.25}$ films it must be emphasized that

the behavior at lower temperatures of F_p vs h reported in Fig.s 4 and 5 is somewhat similar to the the data reported on amorphous films of A15 materials, and discussed in the framework of collective pinning mechanism [11]. In this framework, for $T<T_c/2$ temperature, we are in the limit of eq. 11 of [11]. However also the model in [12], based on the plastic deformation of the flux line lattice, can qualitatively account for the observed behavior. Further experiments and quantitative analysis on these results are required to account for the lack of scaling in our samples. Among the reasons that could induce the lack of scaling as described in [13] we exclude: inhomogeneity of the material since the T_c of $Nb_{0.75}Zr_{0.25}$ is not highly sensitive to the composition; paramagnetic limiting of H_{c2}.

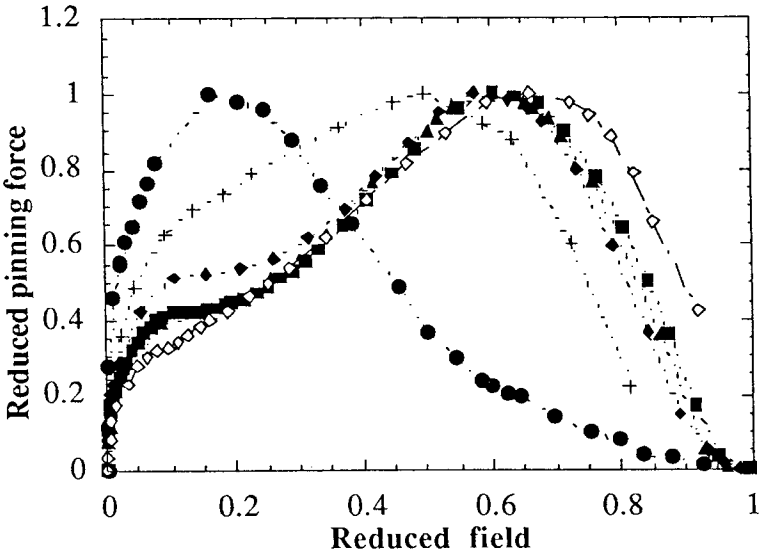

FIG. 5 – F_p vs h at for sample #29A 20 μm line (solid symbols): T= 9.5K (circles) T=6.5 K (rhombs) T=5 K (squares) T=4.2 K (triangles). Crosses and open rhombs refers to #17 respectively for T=8.5 K and T=4.2 K.

IV. CONCLUSION

We realized thin films of $Nb_{0.75}Zr_{0.25}$ in a suitable geometry to perform critical current measurements as a function of the temperature. We estimated the coherence length ξ_0 of the $Nb_{0.75}Zr_{0.25}$ films from the measured $H_{c2}(T)$ which resulted larger than previous results obtained from tunneling measurements.

We have also measured the $J_0(T)$ of the $Nb_{0.75}Zr_{0.25}$ films. The Anderson–Kim theory on the critical current as a function of the temperature is in good agreement with the experimental data and the extrapolated value $J_0(0)$ is not very different from previously reported data.

Finally we analyze the pinning force behavior from transport current measurements in a transverse applied magnetic field. The experiment shows that the maximum pinning force at temperatures near T_c occurs at low reduced fields, $h\approx0.2$, while lowering the temperature the maxima of pinning forces shift quickly towards higher reduced fields, $h\approx0.7$, and keep this almost constant value at different temperatures.

REFERENCES

[1] C. K. Jones, J. K. Hulm, B. S. Chandrasekhar, "Upper critical field of solid solution alloys of the transition elements," Rev. Mod. Phys., 74 (January 1964)

[2] J. K. Hulm, R. D. Blaugher, "Superconducting solid solution alloys of the transition elements," Phys. Rev. **123**, 1569 (1961)

[3] H. J. Spitzer, J. Vac. Sci. Technol. **7**, "Preparation and superconducting properties of Niobium–Zirconium thin films," 537 (1970)

[4] H. Sekine, K. Inoue, K. Tachikawa, "Structure and superconducting properties of Nb–Zr alloy films made by high rate sputtering," J. Japan Institute of Metals, **42**, 424 (1978)

[5] U. Gambardella, D. Di Gioacchino, G. Paternò, M. Cirillo, "Superconducting properties of $Nb_{0.75}Zr_{0.25}$–oxide–$Nb_{0.75}Zr_{0.25}$ tunnel junctions," J. Low Temp. Phys. **87**, 23 (1992)

[6] N. R. Werthamer, E. Helfand, P. C. Hohenberg, "Temperature and purity dependence of the superconducting critical field, H_{c2}. III. Electron spin and spin–orbit effects," Phys. Rev. **147**, 295 (1966)

[7] R. R. Hake, "Upper critical field limits for bulk type II superconductors," Appl. Phys. Lett. **10**, 189 (1967)

[8] D. Di Gioacchino, P. Fabbricatore, S. Frigerio, U. Gambardella, R. Musenich, R. Parodi, G. Paternò, S. Rizzo, C. Vaccarezza, "DC features and RF losses of Nb–based superconducting thin films," IEEE Trans. on Mag. **27**, 1299 (1991)

[9] L. R. Testardi, L. F. Mattheiss, "Electron lifetime effects on properties of A15 and bcc materials", Phys. Rev. Lett. **41**, 1612 (1978)

[10] E. J. Kramer, "Scaling laws for flux pinning in hard superconductors", J. Appl. Phys.**44** 3, 1360 (1973)

[11] P. H. Kes, C. C. Tsuei, "Two dimensional collettive flux pinning, defects, and structural relaxation in amorphous superconducting films", Phys. Rev. B **28** 9, 5126 (1983)

[12] H. J. Jensen, Y Brechet, A. Brass, "On the threshold pinning force in type II superconducting films", J. Low Temp. Phys. **74**, 293 (1989)

[13] S. A. Alterovitz, J. A. Woollam, "Scaling laws for pinning forces in inhomogeneous superconductors," Philosophical Magazine B **38**, 619 (1978)